Generating simplified ammonia reaction model using genetic algorithm and its integration into numerical combustion simulation of 1 MW test facility

Nakamura, Hisashi
Institute of Fluid Science, Tohoku University

Zhang, Juwei
Technology & Intelligence Integration, IHI Corporation

Hirose, Kaito
Institute of Fluid Science, Tohoku University

Shimoyama, Koji
Institute of Fluid Science, Tohoku University

他

出版情報：Applications in Energy and Combustion Science. 15, pp.100187-, 2023-09. Elsevier
バージョン：

Applications in Energy and Combustion Science 15 (2023) 100187

Contents lists available at ScienceDirect

Applications in Energy and Combustion Science

journal homepage: www.sciencedirect.com/journal/applications-in-energy-and-combustion-science

Generating simplified ammonia reaction model using genetic algorithm and its integration into numerical combustion simulation of 1 MW test facility

Hisashi Nakamura [a,*], Juwei Zhang [b,*], Kaito Hirose [a,c], Koji Shimoyama [a,d], Takamasa Ito [b], Tralin Kanaumi [b]

[a] Institute of Fluid Science, Tohoku University, 2-1-1 Katahira, Aoba-ku, Sendai, Miyagi, 980-8577, Japan
[b] Technology & Intelligence Integration, IHI Corporation, Shin-nakahara-cho, 1, Isogo-ku, Yokohama, 235-8501, Japan
[c] Department of Mechanical Systems Engineering, Graduate School of Engineering, Tohoku University, 6-6, Aramaki Aza Aoba, Aoba-ku, Sendai, Miyagi, 980-8579, Japan
[d] Department of Mechanical Engineering, Kyushu University, 744 Motooka, Nishi-ku, Fukuoka, 819-0395, Japan

ARTICLE INFO

Keywords:
Genetic algorithm
Inverse problem
Ammonia combustion
Boiler
CFD simulations
Nitric oxide (NO)

ABSTRACT

A small reaction model for ammonia is necessary for the design and development of large-scale ammonia combustion systems using computational fluid dynamics (CFD) simulation. The present study generated a simplified reaction model for ammonia using a genetic algorithm (14 species and 45 reactions). Optimization was applied to reproduce the combustion properties of ignition delay times, mole fractions of ammonia and nitric oxide at the exit of a single perfectly stirred reactor (PSR), those of a two-staged PSR, and laminar flame speed. The generated simplified reaction model for ammonia was applied to combustion CFD simulation for a 1 MW boiler test facility. Results of CFD simulation reproduced the characteristics of two-staged combustion well. Nitrous oxide emissions predicted by the simulation agreed well with experimental results.

Introduction

As a carbon neutral next-generation fuel, ammonia is expected to play an important role in the fight against with global warming. Ammonia, which can be used as a carrier of hydrogen, has merits of high hydrogen density, a high boiling point, existing infrastructure for production, and much easier transportation than that for hydrogen. Ammonia co-firing technologies are applicable to boilers, gas turbines, engines, industrial furnaces, etc. Among these, IHI corporation has devoted its efforts since 2017 to the R&D of ammonia/coal co-firing technologies in boilers by experiments [1,2], reaction analyses [3,4], and computational fluid dynamics (CFD) simulations [2,5]. Usually, CFD is regarded as an effective approach for evaluating the performance of large-scale boilers. Nevertheless, it is unrealistic to perform CFD simulations using detailed reaction models for ammonia because of the high calculation costs. The detailed reaction models for ammonia are much smaller than those for hydrocarbons but are still too large to be applicable to CFD simulation for large-scale boilers. Consequently, a simplified ammonia reaction model must be built for the CFD simulation of large-scale boilers.

Various methods of reducing the size of detailed reaction models have been proposed [6–11]. A direct relative graph (DRG) method [7] has been extensively utilized to generate reduced reaction models for various fuels. DRG method eliminates unimportant species and reactions under given test conditions from a detailed reaction model. Liu and Han [12] applied the DRG method with sensitivity analysis to reproduce the explosion limits of ammonia and ammonia/hydrogen blends. The detailed reaction model developed by Mei et al. [13] (38 species and 265 reactions) was reduced to 26 species and 82 reactions. An even smaller ammonia reaction model is necessary for the practical combustion simulations of large-scale boilers. In addition to oxidation, formation and reduction of nitric oxide (NO) are necessary for test conditions because the prediction performance for NO is essential to a reaction model used in boiler CFD simulations. However, it is generally challenging that a smaller ammonia reaction model is generated using DRG method for multiple combustion properties.

The present study proposes a method to generate a simplified ammonia reaction model using a genetic algorithm (GA). Because of the effectiveness and robustness of GA for nonlinear problems, the optimization of rate parameters using GA has been applied for reduced reaction

* Corresponding authors.
E-mail addresses: hisashi.nakamura@tohoku.ac.jp (H. Nakamura), zhang0576@ihi-g.com (J. Zhang).

https://doi.org/10.1016/j.jaecs.2023.100187
Received 4 April 2023; Received in revised form 20 July 2023; Accepted 31 July 2023
Available online 1 August 2023

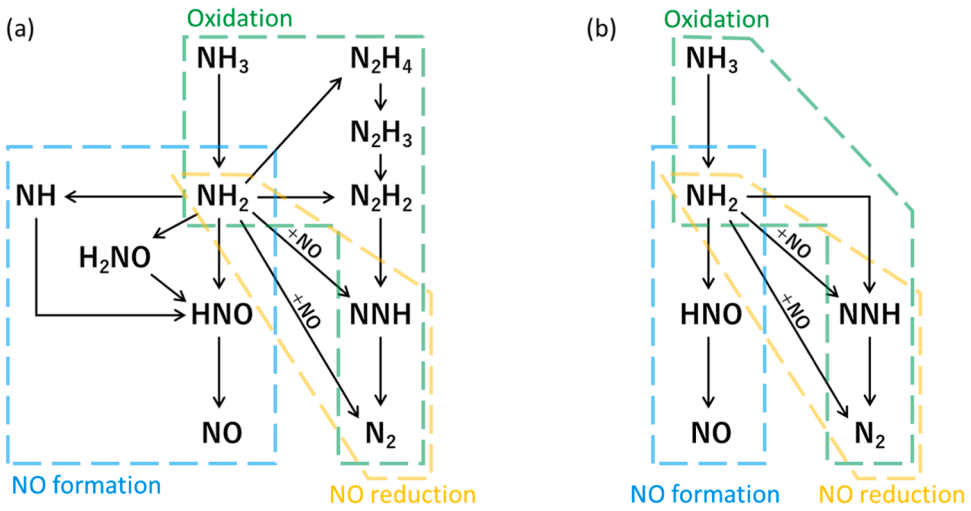

Fig. 1. Schematic of ammonia reaction pathways, (a) detailed and (b) abbreviated.

models [14–19] and global reaction models [20–22]. Elliott et al. [14] optimized the rate parameters of reduced reaction mechanisms to reproduce species mole fractions in a perfectly stirred reactor (PSR) and a burner-stabilized flame. Montgomery et al. [15] applied a GA to select the optimum QSS species in ignition problems. Perini et al. [16] developed a method using a GA combined with mechanism reduction for ignition problems. Sikalo et al. [17] introduced a penalty function to improve the effectiveness of rate parameter optimization in reduced reaction mechanisms for ignition problems. Jaouen et al. [18] proposed a method combining a GA with DGREP and QSS. They demonstrated its capability for methane/vitiated-air flames. Chang et al. [19] used GA optimization for rate parameters of C4–C5 sub-reactions in an *n*-pentanol reduced mechanism to reproduce ignition delay times and species concentrations in a jet-stirred reactor (JSR). For GA applications to global reaction models, Polifke et al. [20] applied GAs for optimizing the rate parameters of two-step and three-step global reaction mechanisms to reproduce heat release rates in 1-D flames. Cailler et al. [21] introduced non-Arrhenius parameters to a two-step global reaction mechanism and applied GA optimization to reproduce flame temperature dependence on an equivalence ratio. Hamosfakidis and Reitz [22] developed an eight-step global reaction mechanism for a diesel component. Its rate parameters were optimized using a GA to reproduce ignition delays. Because of the simplicity of such global reaction mechanisms, however, optimizing multiple combustion properties are expected to be difficult.

The present study sets abbreviated reaction pathways of ammonia combustion with small numbers of species and reactions. Furthermore, GA optimization is applied to rate parameters in abbreviated reaction pathways to reproduce characteristics of ammonia oxidation and NO formation and reduction. A simplified ammonia reaction model generated by the present method is demonstrated in combustion CFD simulations for a boiler test facility.

Simplified ammonia reaction model

Fig. 1a, depicts a schematic of a detailed reaction pathway for ammonia [23]. Following NH_2 radical formation by H-atom abstraction reaction of ammonia, three major pathways for NH_2 radical consumption exist: oxidation, NO formation, and NO reduction. In the oxidation pathway, the NH_2 radical recombination channel produces N_2H_2 and N_2H_4. These N_2H_x species go to NNH by losing a H atom; NNH finally decomposes to N_2. In the NO formation pathway, a NH_2 radical reacts with H_2–O_2 radicals (mostly with an O radical) and forms HNO. HNO is also formed through NH and H_2NO from NH_2. NO is formed from NHO with H_2–O_2 radicals and O_2. In the NO reduction pathway, NH_2 + NO reactions form NNH or N_2. Fig. 1a shows that three species, NH_2, HNO, and NNH show high degrees in the graph and play the role of "hub" in the three major pathways. In the present study, we set abbreviated reaction pathways using the three hub species, reactant (NH_3), and products (NO and N_2), as portrayed in Fig. 1b. Furthermore, a simplified ammonia reaction model was generated using the following procedure:

Table 1
Nitrogen reactions whose rate constants are taken from the base reaction model.

NH2 + O = HNO + H
NH2 + NO = NNH + OH
NH2 + NO = N2 + H2O
NNH + M = N2 + H + M
HNO + O2 = HO2 + NO

Table 2
Virtual reactions whose rate constants were optimized using GA.

NH3 + OH = NH2 + H2O	HNO + H = NO + H2
NH3 + O = NH2 + OH	HNO + OH = NO + H2O
NH3 + H = NH2 + H2	HNO + O = NO + OH
NH3 + HO2 = NH2 + H2O2	HNO + HO2 = NO + H2O2
NH2 + H + M = NH3 + M	NNH + OH = N2 + H2O
NH2 + OH = HNO + H2	NNH + H = N2 + H2
NH2 + HO2 = HNO + H2O	NNH + O = N2 + OH
NH2 + NH2 = NNH + H2 + H	NNH + HO2 = N2 + H2O2
NH2 + NH2 = N2 + H2 + 2H	

(1) A detailed reaction model in [23] is used as the base reaction model.
(2) H_2–O_2 reactions are taken from the base reaction model as they are.
(3) Reactions shown in Table 1 are taken from the base reaction model as they are because of the largest rate of production in the abbreviated reaction pathways.
(4) Virtual reactions in Table 2 are considered. Their rate constants are optimized by GA to reproduce combustion properties in test conditions.
(5) Thermodynamic and transport data are taken from the base reaction model as they are.

The vertical reactions were chosen as NH_3 + X, NH_2 + X, HNO + X, and NNH + X reactions, where X represents H_2–O_2 radicals (H, O, OH, and HO_2). To mimic the NH_2 radical recombination reaction and its subsequent pathways, $NH_2 + NH_2 = NNH + H_2 + H$ and $NH_2 + NH_2 =$

Table 3
Test conditions of combustion properties.

(a) IDT: adiabatic, closed homogeneous reactor at constant volume

Mixture	Initial T (K)	ϕ	Initial P (atm)
NH_3/air	2000	1.0	1.0
	1333		
	1000		
	2000	2.0	
	1333		
	1000		
	2000	0.5	
	1333		
	1000		

(b) $PSR1_{NO}$ and $PSR1_{NH3}$: Single open homogeneous reactor at constant temperature and volume (residence time: 1 s; inlet temperature: 300 K)

Mixture	Reactor T (K)	ϕ	Reactor P (atm)
NH_3/air	1500	0.6	1.0
		0.8	
		1.0	
		1.1	
		1.2	
		1.3	
		1.4	
	2000	0.6	
		0.8	
		1.0	
		1.1	
		1.2	
		1.3	
		1.4	

(c) $PSR2_{NO}$ and $PSR2_{NH3}$: Two-staged open homogeneous reactor at constant temperature and volume (residence time at first stage: 1 s; residence time at second stage: 2 s, inlet temperature: 300 K, reactor temperature at second stage: $T - 300$)

Mixture	Reactor T at first stage (K)	Overall ϕ	Reactor P (atm)	Two-stage combustion ratio, R_s
NH_3/air	1300	0.85	1.0	0.20
	1500			
	1700			
	1900			
	1300			0.35
	1500			
	1700			
	1900			

(d) LFS: Adiabatic 1-D steady planar flame

Mixture	Inlet T (K)	ϕ	P (atm)
NH_3/air	300	1.0	1.0

$N_2 + H_2 + 2H$ were also included in the virtual reactions. The total size of the present simplified ammonia reaction model was 14 species and 45 reactions. The present methodology is an inverse problem compared with mechanism reductions: a minimal set of reaction equations (pathways) is an input in the present method, whereas it is an output in mechanism reductions. It is noteworthy that N_2O reactions were not considered in the present study because of high-temperature process with long residence time in the present combustion facility.

The objective function to be minimized, f, was evaluated using combustion properties computed with the base reaction model and the simplified reaction model. Ignition delay time (IDT), NO and NH_3 mole fractions at the exit of a single perfectly stirred reactor ($PSR1_{NO}$ and $PSR1_{NH3}$, respectively), NO and NH_3 mole fractions at the exit of a two-staged perfectly stirred reactor ($PSR2_{NO}$ and $PSR2_{NH3}$, respectively), and laminar flame speed (LFS) were used as combustion properties. The objective function for the combustion property i, f_i, was defined as

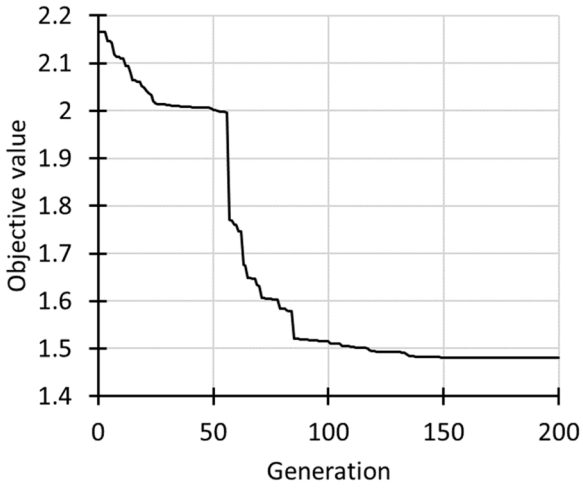

Fig. 2. History of the minimum objective value in the population.

$$f_i = \sqrt{\frac{1}{N_i}\sum_{j=1}^{N_i}\left(\log_{10}\frac{i_{s,j}}{i_{b,j}}\right)^2} \tag{1}$$

where N_i represents the number of test conditions for the combustion property i, $i_{s,j}$ denotes the combustion property computed with the simplified reaction model at the jth test condition, and $i_{b,j}$ stand for the combustion property computed with the base reaction model at the jth test condition. A smaller f_i represents a smaller prediction error of the simplified reaction model to the base reaction model for the target combustion property i. The objective function f was defined as the linear recombination of f_i:

$$f = f_{IDT} + f_{PSR1_{NO}} + f_{PSR1_{NH3}} + f_{PSR2_{NO}} + f_{PSR2_{NH3}} + f_{LFS} \tag{2}$$

Table 3 presents the test conditions of combustion properties chosen as typical conditions of boilers. Computations of the combustion properties were made using Cantera 2.5.1. When computations of $i_{s,j}$ took a long time or failed, a large value was set for $i_{s,j}$.

A MATLAB code was developed to generate the simplified reaction model that minimized the objective function. A GA function in the global optimization toolbox of MATLAB R2020b (The MathWorks Inc.) was used to implement the optimization. To apply GA to a chemical reaction system, one simplified reaction model corresponded to an individual in the population. Each individual was involved with 51 rate parameters to be optimized (17 virtual reactions × 3 Arrhenius parameters per reaction), i.e., the present optimization considered 51 design variables. Initial values of the design variables were given as random values. A Gaussian distribution with mean of 0 and standard deviation of 10 was used to obtain the random values. Conversions from a design variable v to an Arrhenius parameter were applied as follows: 10^v for a pre-exponential factor, $0.01v$ for a temperature exponent, and $|1000v|$ for activation energy in cm^3-mol-cal-s units. These conversions proposed in this study cover a wide range of realistic rate constant and avoid unrealistic rate parameters from random values (e.g. a negative pre-exponential factor and an overly large temperature exponent). The population size was set as 300. The elite fraction and crossover rate were set as 0.05 and 0.8, respectively. Therefore, the top 15 simplified reaction models in the population were guaranteed to survive to the next generation. Crossover was applied to 240 simplified reaction models in the population as parents and created child models by exchanging the design variables of a pair of the parents. Mutation was also applied to 45 simplified reaction models in the population as parents and created child models by introducing random values to design variables of the parents. The same procedure used for the initialization process was used for the mutation process.

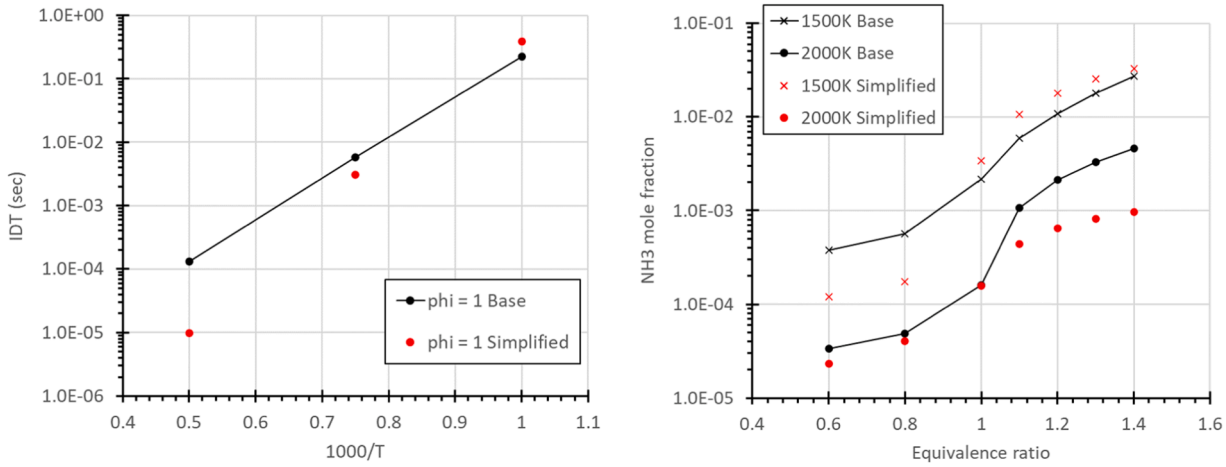

Fig. 3. IDT and $PSR1_{NH3}$ computed the base reaction model and the generated simplified reaction model.

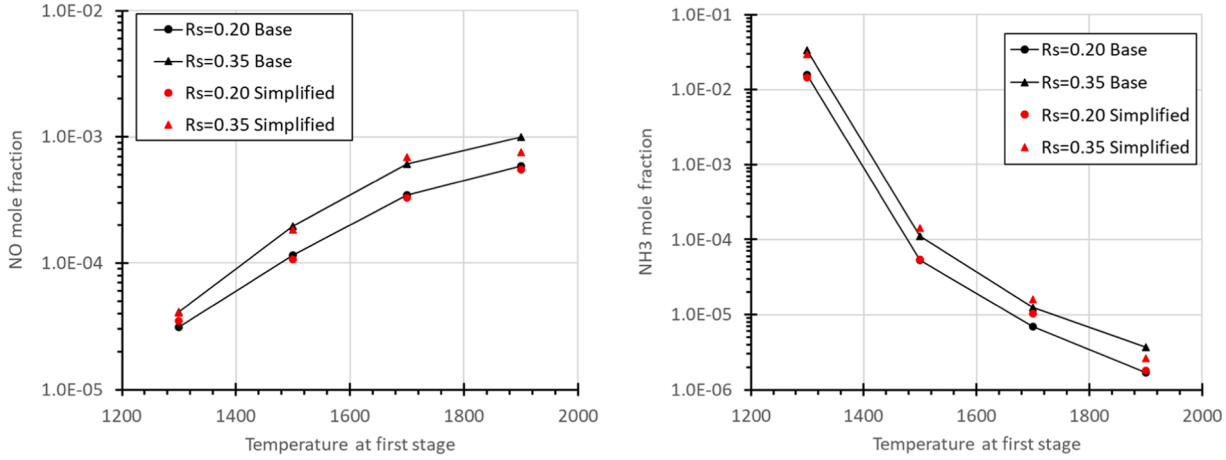

Fig. 4. $PSR2_{NO}$ and $PSR2_{NH3}$ computed the base reaction model and the generated simplified reaction model. (R_s: two-stage combustion ratio).

Fig. 2 presents the history of the minimum objective value in the population. The minimum objective value decreases with the number of generations. Large drops of the minimum objective values are observed at several generations (57th, 63rd, and 85th). The minimum objective value becomes almost constant after the 150th generation. The individual with the minimum objective value at the 200th generation is used as the generated simplified ammonia reaction model hereinafter. The objective values of the combustion properties of the generated simplified ammonia reaction model were $f_{IDT} = 0.69$, $f_{PSR1_{NO}} = 0.25$, $f_{PSR1_{NH3}} = 0.37$, $f_{PSR2_{NO}} = 0.05$, $f_{PSR2_{NH3}} = 0.10$, and $f_{LFS} = 0.001$.

Fig. 3 shows IDT and $PSR1_{NH3}$ computed with the base reaction model and the generated simplified reaction model. IDT and $PSR1_{NH3}$ showed relatively higher objective values compared to the other combustion properties. IDT computed with the generated simplified reaction model is shorter than that with the base reaction model at 2000 K. $PSR1_{NH3}$ computed with the generated simplified reaction model are lower than those with the base reaction model in lean conditions at 1500 K and in fuel-rich conditions at 2000 K. As a result, the objective values of IDT and $PSR1_{NH3}$ are relatively higher than those of the other combustion properties. More species and reactions would be necessary for smaller objective values of IDT and $PSR1_{NH3}$. However, the generated simplified reaction model still captures qualitative trends of IDT to temperature and $PSR1_{NH3}$ to equivalence ratio. Fig. 4 shows $PSR2_{NO}$ and $PSR2_{NH3}$ computed with the base reaction model and the generated simplified reaction model. $PSR2_{NO}$ and $PSR2_{NH3}$ showed relatively lower objective values compared to the other combustion properties.

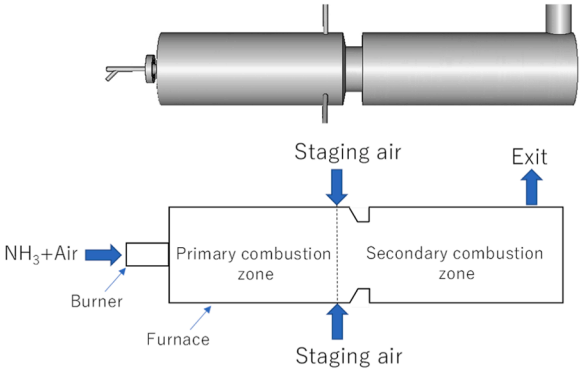

Fig. 5. Outline of the combustion facility.

The generated simplified reaction model satisfactorily reproduces NO and NH_3 emissions predicted with the base reaction model in two-staged combustion. The generated simplified reaction model was applied to combustion CFD simulations. The methods and results of combustion CFD simulations are presented in the next section.

Combustion simulation for 1 MW test facility

The generated simplified ammonia reaction model was evaluated by

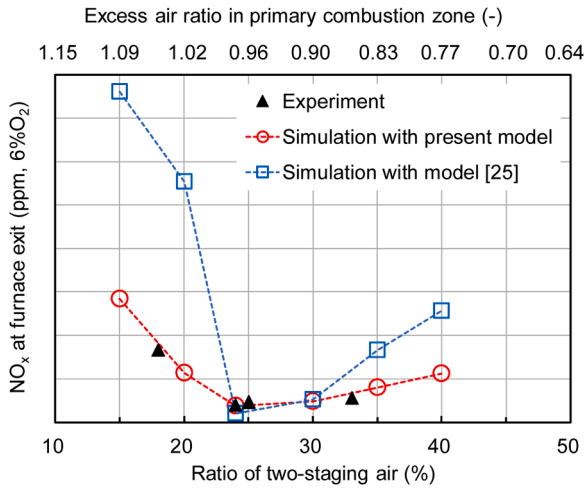

Fig. 6. Comparison between experimental and CFD simulation results (NOx in experiment included NO and NO_2, whereas NOx in computations used NO).

CFD simulation of ammonia combustion experiments in a combustion facility with a rated heat input of 1.0 MW. An outline of this facility is presented in Fig. 5. Ammonia and air were introduced to a burner depicted on the left side of Fig. 5. To reduce NOx emissions, a two-stage combustion method was adopted, with a portion of the air being introduced to the middle of the furnace. Therefore, the furnace was divided into a primary combustion zone and a secondary combustion zone. The NO_x mole fraction at the furnace exit was measured using a gas analyzer with nondispersive infrared (NDIR) absorption.

The CFD simulation was performed using ANSYS FLUENT 20. The generated simplified ammonia reaction model was integrated into the simulation. The adopted turbulence model was Realizable k-ε because of its superior performance for flow involving rotation. The turbulence-chemistry interaction was based on the Eddy-Dissipation Concept (EDC). To match the experimental conditions, the CFD simulation was performed with heat input of 0.84 MW and a total excess air ratio of 1.28. The excess air ratios in the primary zone were set in the range of 0.77 to 1.09, corresponding to a two-stage combustion ratio (the proportion of the secondary air amount to the total air amount) of 15% to 40%. The inputs of fuel and air were approximately 164 kg/h and 972 kg/h. The wall temperature was set as 40 °C, which was the temperature of the cooling water. The number of meshes was around 424 million, which was considered as sufficiently fine for the present combustion facility, based findings from an earlier study [24].

The applicability of the generated simplified ammonia reaction model was confirmed in the CFD simulation. Fig. 6 presents a comparison of values found from the simulation and from experimentation to assess the NOx mole fractions at the furnace exit under various conditions. The change in NOx mole fractions at the furnace exit attributable to the excess air ratio in the primary combustion zone (or two-stage combustion ratio) obtained using the CFD simulation agreed well with the experiment. This simulation result was greatly improved compared to results calculated using the Okafor's reaction model [25] in the case of NH_3 firing, except for co-firing with methane. Therefore, the accuracy of CFD simulation adopting the generated simplified ammonia reaction model was confirmed. In addition, Fig. 6 showed that both the simulation and experiment indicated a "V"-shaped trend in NOx mole fraction responses to the two-stage combustion ratio, and it was found that the minimum value of NOx mole fraction appeared near an excess air ratio of around 0.95 in the primary combustion zone (slightly fuel-rich). Results demonstrated that the NOx mole fraction increased suddenly when the excess air ratio exceeds 1.0, i.e., on the fuel-lean side.

The cause of the previously described of NOx can be inferred from Figs. 7 and 8, which show the distributions of gas temperature, NO and ammonia mole fractions, and reaction rate of NH_2 with OH in the furnace. The temperature distributions in Fig. 7(a) display good ignitability under all conditions. Results showed a higher flame temperature in the primary combustion zone than in the secondary combustion zone. Combustion in the primary combustion zone became more intense as the primary air ratio approached 1.0. In addition, in the three fuel-rich conditions (excess air ratios of 0.77, 0.83, and 0.90 in the primary combustion zone) where the residual ammonia remained in the primary region, a significant increase in temperature attributable to ammonia after-burning was observed when the staging combustion air was introduced. The mole fraction distribution of NO in Fig. 7(b) showed that, under fuel-lean conditions (excess air ratio higher than 1.0), NO generated in the flame could not be reduced because the entire furnace including both the primary and secondary combustion zones was in a fuel-lean state and was discharged as is. However, in the three fuel-rich

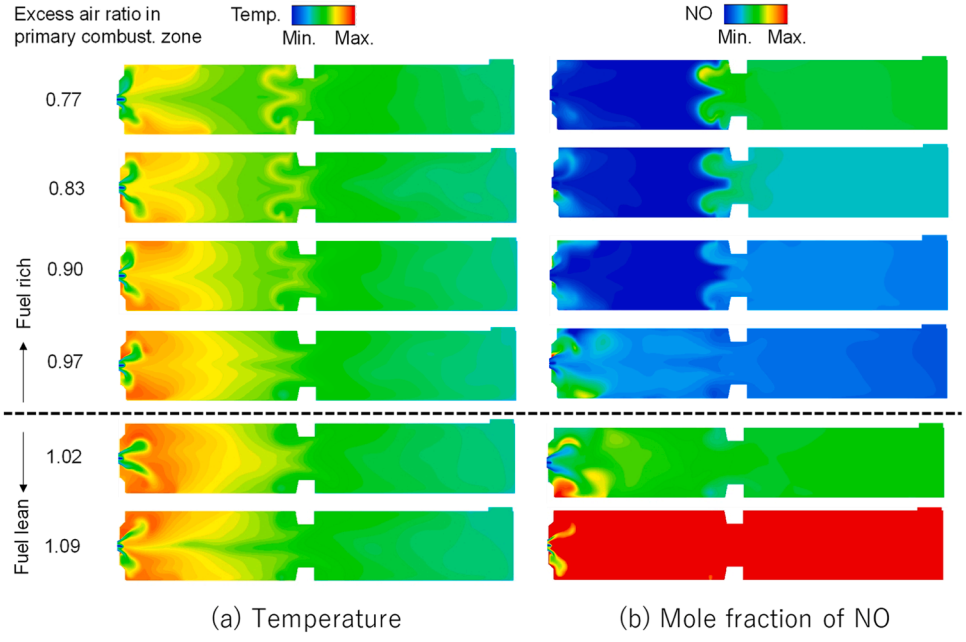

Fig. 7. Gas temperature distribution and mole fraction distribution of NO obtained from CFD simulation.

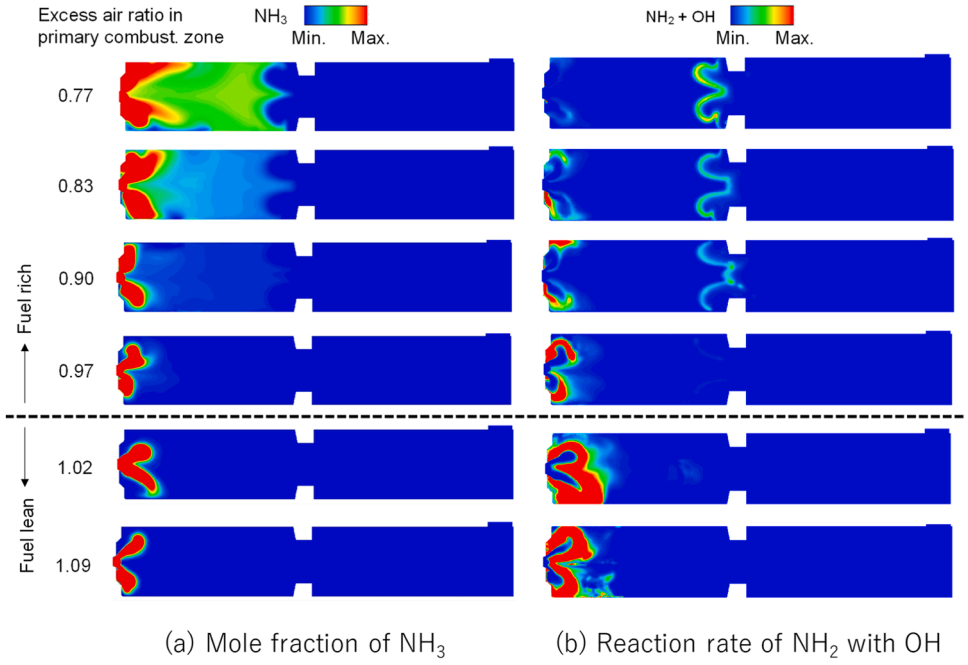

Fig. 8. Mole fraction distribution of NH_3 and oxidation rate distribution of NH_2 obtained from CFD simulation.

conditions (excess air ratios of 0.77, 0.83, and 0.90), NO in the primary combustion zone was reduced almost to zero. The amount of NO generated by ammonia after-burning increased when staging combustion air was introduced. Moreover, under slightly fuel-rich conditions (excess air ratio of 0.97), results demonstrated that the inhibition of NO from both the flame and ammonia after-burning were achieved, resulting in the lowest NO mole fraction at the furnace exit.

The mole fraction distributions of ammonia in Fig. 8(a) showed that, under fuel-lean conditions (excess air ratio higher than 1.0), ammonia was consumed almost to zero in the flame. By contrast, results obtained under fuel-rich conditions indicated that residual ammonia after the flame increased as the excess air ratios in the primary combustion zone decreases. According to the distribution of the reaction rate of NH_2 with OH in Fig. 8(b), results showed that, under fuel-lean conditions (excess air ratio above 1.0), there was almost no residual ammonia after the flame. Therefore, injecting a staging combustion air did not cause any ammonia after-burning. By contrast, under fuel-rich conditions, as the excess air ratio in the primary zone decreased, the residual ammonia after combustion increased. Consequently, the results demonstrated that after-burning of ammonia became increasingly remarkable.

Conclusions

A simplified reaction model for ammonia combustion with 14 chemical species and 45 reactions was generated using a genetic algorithm. The CFD simulation by integrating this reaction model was performed for ammonia combustion experiments in a combustion furnace. Results showed that the change in NOx mole fraction at the furnace exit to two-stage combustion ratio was in good agreement with the experimental values. In addition, results demonstrated that when the condition of the primary combustion zone was slightly fuel-rich (e.g., excess air ratio of about 0.95), inhibition of both the NOx from the flame and from the after-burning of ammonia was achieved, resulting in a minimum value of NOx concentration at the furnace exit. These ammonia combustion characteristics are expected to be useful for the design and operation of ammonia combustion burners.

Declaration of Competing Interest

The authors declare that they have no known competing financial interests or personal relationships that could have appeared to influence the work reported in this paper.

Data availability

The data that has been used is confidential.

Acknowledgement

This study was partially supported by JSPS KAKENHI Grant number 20H02077.

References

[1] Nagatani G, Ishii H, Ito T, Ohno E, Okuma Y. Development of co-firing method of pulverized coal and ammonia to reduce greenhouse gas emissions. IHI Eng Rev 2020;53:1–10.
[2] Tamura M, Gotou T, Ishii H, Riechelmann D. Experimental investigation of ammonia combustion in a bench scale 1.2 MW-thermal pulverised coal firing furnace. Appl Energy 2020;277:115580. https://doi.org/10.1016/j.apenergy.2020.115580.
[3] Ishihara S, Zhang J, Ito T. Numerical calculation with detailed chemistry on ammonia co-firing in a coal-fired boiler: effect of ammonia co-firing ratio on NO emissions. Fuel 2020;274:117742. https://doi.org/10.1016/j.fuel.2020.117742.
[4] Ishihara S, Zhang J, Ito T. Numerical calculation with detailed chemistry of effect of ammonia co-firing on NO emissions in a coal-fired boiler. Fuel 2020;266:116924. https://doi.org/10.1016/j.fuel.2019.116924.
[5] Zhang J, Ito T, Ishii H, Ishihara S, Fujimori T. Numerical investigation on ammonia co-firing in a pulverized coal combustion facility: effect of ammonia co-firing ratio. Fuel 2020;267:117166. https://doi.org/10.1016/j.fuel.2020.117166.
[6] Lu T, Ju Y, Law CK. Complex CSP for chemistry reduction and analysis. Combust Flame 2001;126:1445–55. https://doi.org/10.1016/S0010-2180(01)00252-8.
[7] Lu T, Law CK. A directed relation graph method for mechanism reduction. Proc Combust Inst 2005;30:1333–41. https://doi.org/10.1016/j.proci.2004.08.145.
[8] Pepiot-Desjardins P, Pitsch H. An efficient error-propagation-based reduction method for large chemical kinetic mechanisms. Combust Flame 2008;154:67–81. https://doi.org/10.1016/j.combustflame.2007.10.020.
[9] Niemeyer KE, Sung C-J, Raju MP. Skeletal mechanism generation for surrogate fuels using directed relation graph with error propagation and sensitivity analysis. Combust Flame 2010;157:1760–70. https://doi.org/10.1016/j.combustflame.2009.12.022.

[10] Sun W, Chen Z, Gou X, Ju Y. A path flux analysis method for the reduction of detailed chemical kinetic mechanisms. Combust Flame 2010;157:1298–307. https://doi.org/10.1016/j.combustflame.2010.03.006.
[11] Ranzi E, Dente M, Goldaniga A, Bozzano G, Faravelli T. Lumping procedures in detailed kinetic modeling of gasification, pyrolysis, partial oxidation and combustion of hydrocarbon mixtures. Prog Energy Combust Sci 2001;27:99–139. https://doi.org/10.1016/S0360-1285(00)00013-7.
[12] Liu Y, Han D. Numerical study on explosion limits of ammonia/hydrogen/oxygen mixtures: sensitivity and eigenvalue analysis. Fuel 2021;300:120964. https://doi.org/10.1016/j.fuel.2021.120964.
[13] Mei B, Zhang X, Ma S, Cui M, Guo H, Cao Z, Li Y. Experimental and kinetic modeling investigation on the laminar flame propagation of ammonia under oxygen enrichment and elevated pressure conditions. Combust Flame 2019;210:236–46. https://doi.org/10.1016/j.combustflame.2019.08.033.
[14] Elliott L, Ingham DB, Kyne AG, Mera NS, Pourkashanian M, Wilson CW. Genetic algorithms for optimisation of chemical kinetics reaction mechanisms. Prog Energy Combust Sci 2004;30:297–328. https://doi.org/10.1016/j.pecs.2004.02.002.
[15] Montgomery CJ, Yang C, Parkinson AR, Chen J-Y. Selecting the optimum quasi-steady-state species for reduced chemical kinetic mechanisms using a genetic algorithm. Combust Flame 2006;144:37–52. https://doi.org/10.1016/j.combustflame.2005.06.011.
[16] Perini F, Brakora JL, Reitz RD, Cantore G. Development of reduced and optimized reaction mechanisms based on genetic algorithms and element flux analysis. Combust Flame 2012;159:103–19. https://doi.org/10.1016/j.combustflame.2011.06.012.
[17] Sikalo N, Hasemann O, Schulz C, Kempf A, Wlokas I. A genetic algorithm–based method for the optimization of reduced kinetics mechanisms. Int J Chem Kinet 2015;47:695–723. https://doi.org/10.1002/kin.20942.
[18] Jaouen N, Vervisch L, Domingo P, Ribert G. Automatic reduction and optimisation of chemistry for turbulent combustion modelling: impact of the canonical problem. Combust Flame 2017;175:60–79. https://doi.org/10.1016/j.combustflame.2016.08.030.
[19] Chang Y, Jia M, Niu B, Xu Z, Liu Z, Li Y, Xie M. Construction of a skeletal oxidation mechanism of n-pentanol by integrating decoupling methodology, genetic algorithm, and uncertainty quantification. Combust Flame 2018;194:15–27. https://doi.org/10.1016/j.combustflame.2018.04.012.
[20] Polifke W, Geng W, Döbbeling K. Optimization of rate coefficients for simplified reaction mechanisms with genetic algorithms. Combust Flame 1998;113:119–34. https://doi.org/10.1016/S0010-2180(97)00212-5.
[21] Cailler M, Darabiha N, Veynante D, Fiorina B. Building-up virtual optimized mechanism for flame modeling. Proc Combust Inst 2017;36:1251–8. https://doi.org/10.1016/j.proci.2016.05.028.
[22] Hamosfakidis V, Reitz RD. Optimization of a hydrocarbon fuel ignition model for two single component surrogates of diesel fuel. Combust Flame 2003;132:433–50. https://doi.org/10.1016/S0010-2180(02)00489-3.
[23] Nakamura H, Hasegawa S, Tezuka T. Kinetic modeling of ammonia/air weak flames in a micro flow reactor with a controlled temperature profile. Combust Flame 2017;185:16–27. https://doi.org/10.1016/j.combustflame.2017.06.021.
[24] Tamura M, Gotou T, Ishii H, Riechelmann D. Experimental investigation of ammonia combustion in a bench scale 1.2 MW-thermal pulverised coal firing furnace. Appl Energy 2020;277:115580. https://doi.org/10.1016/j.apenergy.2020.115580.
[25] Okafor EC, Naito Y, Colson S, Ichikawa A, Kudo T, Hayakawa A, Kobayashi H. Experimental and numerical study of the laminar burning velocity of CH4–NH3–air premixed flames. Combust Flame 2018;187:185–98. https://doi.org/10.1016/j.combustflame.2017.09.002.